Charge Transfer Effects in Naturally Occurring van der Waals Heterostructures $(PbSe)_{1.16}(TiSe_2)_m$ $(m = 1, 2)$

Q. Yao,[1,2,3] D. W. Shen,[2,4,*] C. H. P. Wen,[1,3] C. Q. Hua,[5] L. Q. Zhang,[3,6] N. Z. Wang,[7] X. H. Niu,[1,3] Q. Y. Chen,[1,3] P. Dudin,[8] Y. H. Lu,[9] Y. Zheng,[5] X. H. Chen,[3,7,10] X. G. Wan,[3,6] and D. L. Feng[1,3]

[1]*State Key Laboratory of Surface Physics, Department of Physics, and Laboratory of Advanced Materials, Fudan University, Shanghai 200433, China*
[2]*State Key Laboratory of Functional Materials for Informatics, Shanghai Institute of Microsystem and Information Technology (SIMIT), Chinese Academy of Sciences, Shanghai 200050, China*
[3]*Collaborative Innovation Centre of Advanced Microstructures, Nanjing 210093, China*
[4]*CAS Center for Excellence in Superconducting Electronics (CENSE), Shanghai 200050, China*
[5]*Department of Physics, Zhejiang University, Hangzhou 310027, China*
[6]*National Laboratory of Solid State Microstructures, College of Physics, Nanjing University, Nanjing 210093, China*
[7]*Hefei National Laboratory for Physical Sciences at Microscale and Department of Physics and Key Laboratory of Strongly-coupled Quantum Matter Physics, University of Science and Technology of China, Hefei 230026, China*
[8]*Diamond Light Source, Harwell Science and Innovation Campus, Didcot OX11 0DE, United Kingdom*
[9]*State Key Lab of Silicon Materials, Zhejiang University, Hangzhou 310027, China*
[10]*High Magnetic Field Laboratory, Chinese Academy of Sciences, Hefei 230031, China*

van der Waals heterostructures (VDWHs) exhibit rich properties and thus has potential for applications, and charge transfer between different layers in a heterostructure often dominates its properties and device performance. It is thus critical to reveal and understand the charge transfer effects in VDWHs, for which electronic structure measurements have proven to be effective. Using angle-resolved photoemission spectroscopy, we studied the electronic structures of $(PbSe)_{1.16}(TiSe_2)_m$ ($m = 1, 2$), which are naturally occurring VDWHs, and discovered several striking charge transfer effects. When the thickness of the $TiSe_2$ layers is halved from $m = 2$ to $m = 1$, the amount of charge transferred increases unexpectedly by more than 250%. This is accompanied by a dramatic drop in the electron-phonon interaction strength far beyond the prediction by first-principles calculations and, consequently, superconductivity only exists in the $m = 2$ compound with strong electron-phonon interaction, albeit with lower carrier density. Furthermore, we found that the amount of charge transferred in both compounds is nearly halved when warmed from below 10 K to room temperature, due to the different thermal expansion coefficients of the constituent layers of these misfit compounds. These unprecedentedly large charge transfer effects might widely exist in VDWHs composed of metal-semiconductor contacts; thus, our results provide important insights for further understanding and applications of VDWHs.

Boosted by then enormous effort put into graphenelike materials, research into artificial materials formed by stacking different two-dimensional (2D) crystals in a desired sequence, the so-called van der Waals heterostructures (VDWHs) have gradually drawn considerable attention [1–6]. The interaction between neighboring 2D crystals is relatively weak, but owing to the atomically flat interfaces and precise crystallographic alignment, electronic orbitals can still protrude across the interfaces and thus affect charge carriers in the adjacent 2D crystals. The resulting charge reconstruction leads to emergent properties distinct from those of its individual components, e.g., the observation of Hofstadter's butterfly [7,8], the fractal quantum hall effect [9,10], and the unconventional diode and photovoltaic effects in MoS_2/WSe_2 heterostructures

[11], which naturally pique both fundamental and technological interest. However, the deterministic placement methods for preparing most artificial VDWHs impede the experimental investigation of the influence of charge transfer on their low-energy electronic structure, which is the key to understanding the underlying mechanism and of important directive significance to further devices based on VDWHs.

Misfit compounds, bulk materials that consist of alternately stacked rock-salt and transition metal chalcogenide layers, belong to naturally occurring VDWHs [12–16]. The neighboring structural subsystems exhibit different symmetry and periodicity, leading to an incommensurate crystal structure bound by weak van der Waals interactions between interleaved layers, as sketched in Fig. 1(a) [17].

These compounds provide a unique opportunity to investigate the manipulation of VDWHs, and in particular the cleavable crystal structure and absence of unwanted interlayer adsorbates enable the direct probing of their intrinsic electronic structure by angle-resolved photoemission spectroscopy (ARPES).

In this Letter, through systematic ARPES measurements and first-principles calculations on the low-lying electronic structure of typical naturally occurring VDWHs $(PbSe)_{1.16}(TiSe_2)_m$ ($m = 1, 2$) (denoted as $m1$ and $m2$ hereinafter), we demonstrate remarkable charge transfer effects that may prove endemic to VDWHs. First, varying the thickness of $TiSe_2$ layers from $m2$ to $m1$ results in the significant increase in the charge transferred at the interfaces, which is accompanied by a dramatic drop in the electron-phonon coupling (EPC) strength far beyond the prediction by first-principles calculations. Furthermore, an unexpected temperature-dependent band shift is revealed, which introduces an up to 40% decrease in the charge transfer when warmed from 10 K to room temperature. Since a large number of current prototype VDWH devices are made from transition metal chalcogenides, and their design is optimized mainly based on their low-temperature properties, this finding may prove crucial to the further exploration of VDWH applications.

High-quality $(PbSe)_{1.16}(TiSe_2)_m$ ($m = 1, 2$) single crystals were synthesized by a chemical vapor transport method as described elsewhere [18]. They could be mechanically exfoliated down to few-layer thickness, forming natural and air-stable VDWHs suitable for device applications (see Supplemental Material [19] for details). ARPES measurements were performed at beam line 5–4 of Stanford Synchrotron Radiation Laboratory, beam line I05-ARPES of Diamond Light Source, and beam line 13U of National Synchrotron Radiation Laboratory (NSRL). These beam lines are all equipped with VG-Scienta R4000 electron analyzers. The overall energy resolution was 10–15 meV depending on the photon energy, and the angular resolution was set to 0.3°. All samples were cleaved under a vacuum better than 5×10^{-11} Torr. The details of first-principles calculations can be found in Supplemental Material [19–23].

We first present the photoemission intensity maps of $m1$ [Fig. 1(c)] and $m2$ [Fig. 1(d)] at the Fermi energy E_F. Both full-scale maps show hexagonal symmetry in accord with the lattice of bulk $1T$-$TiSe_2$. According to the crystal structure of misfit compounds, there should be a sizable possibility for the PbSe layer to be present on the surface. However, neither map shows any fourfold symmetric feature from the PbSe layers in all of our more than a dozen samples. We speculate that the random or incommensurate potential may affect PbSe severely and localize its holes, and its photoemission signal is thus smeared in momentum space.

Both Fermi surface maps exhibit elliptical Fermi pockets around the M point similar to bulk $1T$-$TiSe_2$ [24], but a
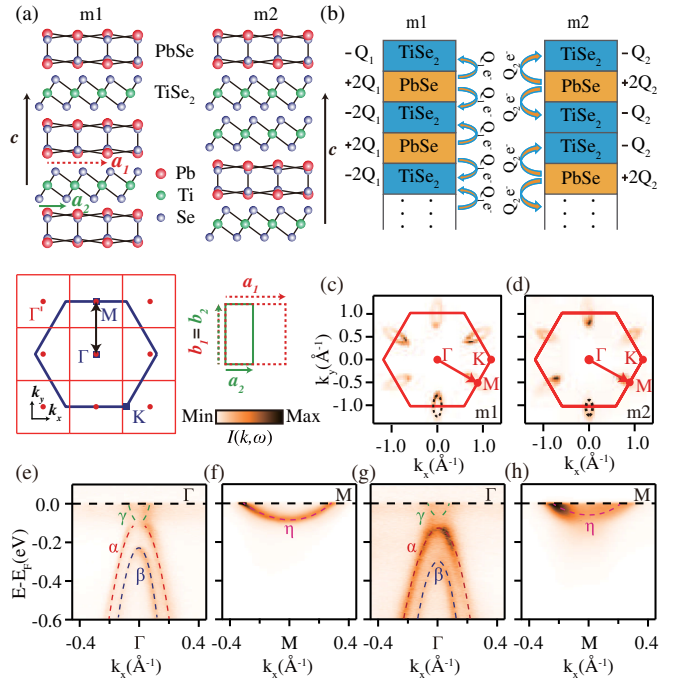

FIG. 1. (a) Crystal structure of $(PbSe)_{1.16}(TiSe_2)_m$ ($m = 1, 2$). The bottom left depicts the projected 2D Brillouin zones (BZ) of the $TiSe_2$ (blue hexagon) and PbSe layers (red squares). Note that the Γ point of the second PbSe BZ and the M point of the $TiSe_2$ layer coincide. The bottom right shows a comparison of their lattice constants. (b) Schematic diagram of the charge transfer at interfaces. Orange and cyan rectangles represent PbSe and $TiSe_2$ layers, respectively. PbSe layers donate electrons to $TiSe_2$ layers. [(c) and (d)] Photoemission intensity maps of $m1$ and $m2$ at E_F, respectively, over the projected 2D BZ. Black dashed ellipses indicate the Fermi pockets and the intensity has been integrated over a window of ($E_F - 2.5$ meV, $E_F + 2.5$ meV). Data were threefold symmetrized. Photoemission intensity plots (e) and (f) for $m1$ and (g) and (h) for $m2$ are presented near Γ and M, respectively. The dashed lines indicate band dispersions obtained from the momentum and energy distribution curves (MDCs and EDCs). All data were taken at 10 K with 80 eV photons.

detailed comparison indicates significant electron doping in both $m1$ and $m2$. The estimated Luttinger volumes of the Fermi pockets are 13% and 7.4% of the Brillouin zone for $m1$ and $m2$, respectively (see more details in Supplemental Material [19]). Based on the charge transfer processes sketched in Fig. 1(b), the doped charge in the surface layer of $m1$ would be half its bulk value, while there is no charge reconstruction in $m2$, which gives bulk doping levels of $0.26 \ e^-$ and $0.074 \ e^-$ per $TiSe_2$ for $m1$ and $m2$, respectively [25–28]. This finding confirms the previous model that the PbSe layers serve as a carrier reservoir for $TiSe_2$ layers, thus giving rise to the charge transfer. When the thickness of the $TiSe_2$ layers is halved from $m2$ to $m1$, the amount of transferred charge increases by as large as 250%, which suggests that varying the thickness of the interleaved layers might provide a rather efficient means of tuning

charge transfer in VDWHs. We note that the charge transfer originates from the difference in Fermi level/ chemical potential of neighboring layers in VDWHs [19]. Although our findings are on bulk misfit compounds, they represent the behaviors of VDWHs down to a few unit cells. As shown by the static electric model analysis in Supplemental Material [19,29], the charge distribution is stable and independent of the number of unit cells down to 2 u.c. of PbSe/TiSe$_2$, 2 u.c. PbSe/TiSe$_2$/TiSe$_2$, or 1 u.c. TiSe$_2$/PbSe/TiSe$_2$.

More detailed electronic structure comparisons of $m1$ and $m2$ are shown in Figs. 1(e)–1(h). In the vicinity of E_F, one electronlike (γ) and two holelike bands (α and β) around Γ together with another electronlike band (η) around M can be clearly resolved. As in the bulk material, η is a Ti $3d$ band while the highly dispersive α and β are spin-orbit-split Se $4p$ bands [30,31]. However, we stress that the γ band in (PbSe)$_{1.16}$(TiSe$_2$)$_m$ cannot be assigned as scattered states by the charge-density-wave (CDW) wave vector as in $1T$-TiSe$_2$, since the CDW is unlikely present in $m1$ and $m2$ for the following reasons. First, throughout the whole temperature range from 300 to 10 K, we have never found any sign of band folding in our ARPES measurements, which is the smoking gun for the presence of bulk or surface CDW states in $1T$-TiSe$_2$ [32]. Secondly, our ARPES measurements have confirmed nearly the same photoemission spectra of $m2$ as those of Cu$_{0.65}$TiSe$_2$, which is located in the same optimal doping regime as $m2$; CDW has been proven absent at this doping [32,33]. Thirdly, the doping level of $m1$ is much higher than $m2$ on the surface, and even higher in the bulk, and thus $m1$ is further away from the CDW regime than $m2$. Instead, γ is more reasonably accounted for as the electronic states of TiSe$_2$ scattered from M by the reciprocal lattice constant of the PbSe layers [illustrated by the double-headed arrow in Fig. 1(a)]. This result suggests that the charge density from the PbSe layers impinges upon the TiSe$_2$ planes, serving as a commensurate potential that scatters the electrons therein [34].

The dramatic change in the transferred charge with m is accompanied by an unexpected modulation of the photoemission spectra of these naturally occurring VDWHs. Figures 2(a) and 2(b) compare EDCs of $m1$ and $m2$ along Γ-M at low temperatures. Note that while the η band of $m1$ shows typical quasiparticlelike dispersion with sharp and well-defined peaks, the spectral line shape of $m2$ taken at the same momenta is remarkably broad and the linewidth is on the same order as the dispersion, which strongly suggests the incoherent nature of the spectra. Meanwhile, the maxima of these incoherent peaks still follow the dispersion predicted by band structure calculations. Taking spectra around the η band bottoms of both compounds as an example [Fig. 2(c)], rather different behavior is clearly observed. The EDC for $m1$ is well fit by a Lorentzian peak having a linewidth of 22.1 meV, in which
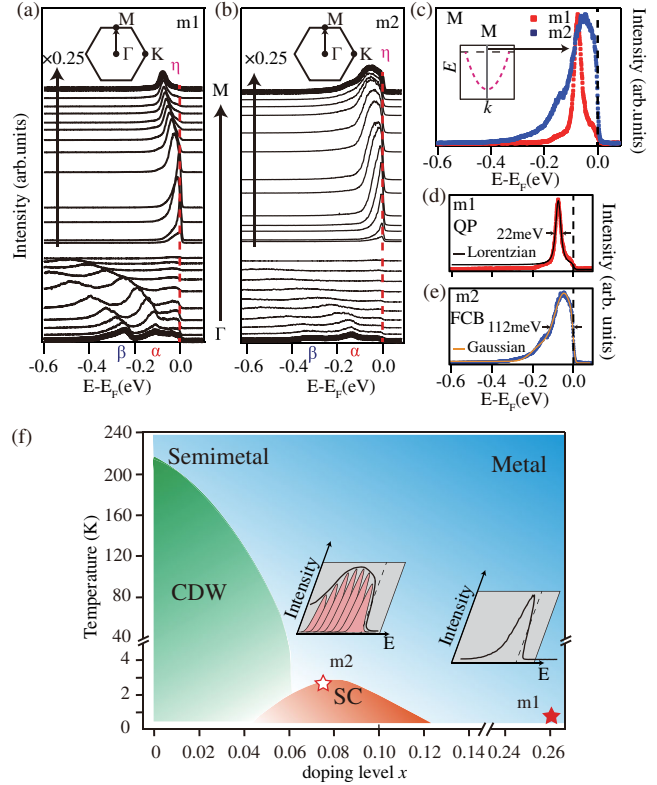

FIG. 2.   [(a) and (b)] EDCs along the Γ-M cuts shown in Figs. 1(c) and 1(d) for $m1$ and $m2$, respectively. Spectra around M have been intentionally scaled down by 0.25 to be comparable to those around Γ. (c) Comparison of their EDCs at the M point. The line shape (d) for $m1$ can be fitted by a Lorentzian peak, while that (e) for $m2$ is fit best by a Gaussian envelope. (f) The phase diagram of electron-doped TiSe$_2$, whose regime below 0.1 doping is reproduced from that of Cu$_x$TiSe$_2$ with one Cu ion doping one electron [33], and the overdoped regime is a sketch. $m1$ is located in the heavily overdoped regime with quasiparticle-like spectra, which extends the original phase diagram, while $m2$ is located in the optimally doped regime and its spectra exhibit the typical Franck-Condon broadening of polarons due to strong EPC.

the shadow band background and the Fermi-Dirac function have been considered [Fig. 2(d)]. In contrast, as shown in Fig. 2(e), the line shape of the spectrum taken from $m2$ is clearly nonquasiparticlelike, and it can only be reasonably fit by a Gaussian function with a linewidth of 112 meV, more than 5 times wider than $m1$. Note that both samples are rather 2D in nature (see Supplemental Material [19] for details, [35]) and transport measurements have further proven the more 2D electronic structure of $m2$. Furthermore, X-ray diffraction and transition electron microscopy have illustrated the similar crystalline quality of our $m1$ and $m2$ samples [18]. Therefore, this unconventional spectroscopic broadening of $m2$ is not due to k_z broadening or disorder. Moreover, since the actual doping in bulk is twice that on the surface for $m1$, its linewidth of bulk states should be even much smaller.

Such spectroscopic linewidth broadening has also been reported at low doping x in Cu_xTiSe_2 [32]—photoemission spectra of $Cu_{0.065}TiSe_2$, located in the same optimal doping regime as $m2$, exhibit an analogous broad feature. The observed sharp Fermi edges in both our data and Ref. [32] represent the Fermi-Dirac cutoff of a broad feature extending well above E_F. This behavior is characteristic of the typical polarons in transition metal chalcogenides [36,37], indicating the very strong EPC in $m2$, which is reasonable as it is in proximity to a CDW phase [38]. In principle, our first-principles calculations can reproduce the tendency for diminishing EPC strength with increasing electron doping in $TiSe_2$, with the coupling constant λ decreasing from 0.55 in $m2$ to 0.51 in $m1$ (see Supplemental Material [19] for more details of calculations, [39–41]). However, the $>500\%$ difference in the spectroscopic linewidth between these two sibling VDWHs is not well accounted for by this calculation, suggesting a much more drastic change in the EPC strength owing to charge transfer. Our findings also suggest that the strong EPC would likely reduce the charge transfer and cause the observed large difference between $m1$ and $m2$—the two $TiSe_2$ layers in $m2$ would share electrons transferred from one layer of PbSe, so that the carrier concentration in its $TiSe_2$ layer would be less than the $m1$ case, which results in stronger EPC that subsequently reduces the charge transfer. This possibility needs to be tested by further calculations including the doping dependent EPC. Moreover, one immediate consequence of such a significant modulation of the EPC is on the emergence of superconductivity in $(PbSe)_{1.16}(TiSe_2)_m$ ($m = 1, 2$). As summarized in the phase diagram of

electron-doped $TiSe_2$ [Fig. 2(f)], the spectra of $m2$ exhibit typical Franck-Condon broadening of polarons due to rather strong EPC, while those of $m1$ behave like the coherent quasiparticle in a weak-coupling regime (see more analysis in Supplemental Material [19]). The weak EPC in $m1$ explains its absence of superconductivity despite the higher density of states near E_F than in $m2$.

Unexpectedly, we discovered that the carrier concentrations of these naturally occurring VDWHs exhibit strong temperature dependence. The upper halves of Fig. 3(a) show the room-temperature photoemission intensity maps of $m1$ and $m2$. Compared with those taken at low temperatures, the electron pockets around M shrink markedly. The more quantitative comparison of Fermi surface contours at different temperatures [the lower part of Fig. 3(a)], extracted from the MDC peak fitting, further confirms that the charge transferred from PbSe to $TiSe_2$ is reduced for both $m1$ and $m2$ on increasing temperature. This shrinking of the Fermi pockets can be attributed to the upward shift of the Ti $3d$ η band [Fig. 3(b)], which could be directly observed from comparisons of EDCs taken at high and low temperatures for $m1$ and $m2$ as well [Figs. 3(c1)–3(c2)]. Detailed temperature dependence measurements indicate that this band shift is continuous and not due to some sudden phase transition, as illustrated in Fig. 3(d). Quantitatively, the η bands of $m1$ and $m2$ shift as much as 24.5 and 21.2 meV towards E_F, respectively, from our lowest measurement temperature to room temperature [Fig. 3(e)].

To account for the temperature-dependent energy shift of the η band, we have considered the thermal expansion
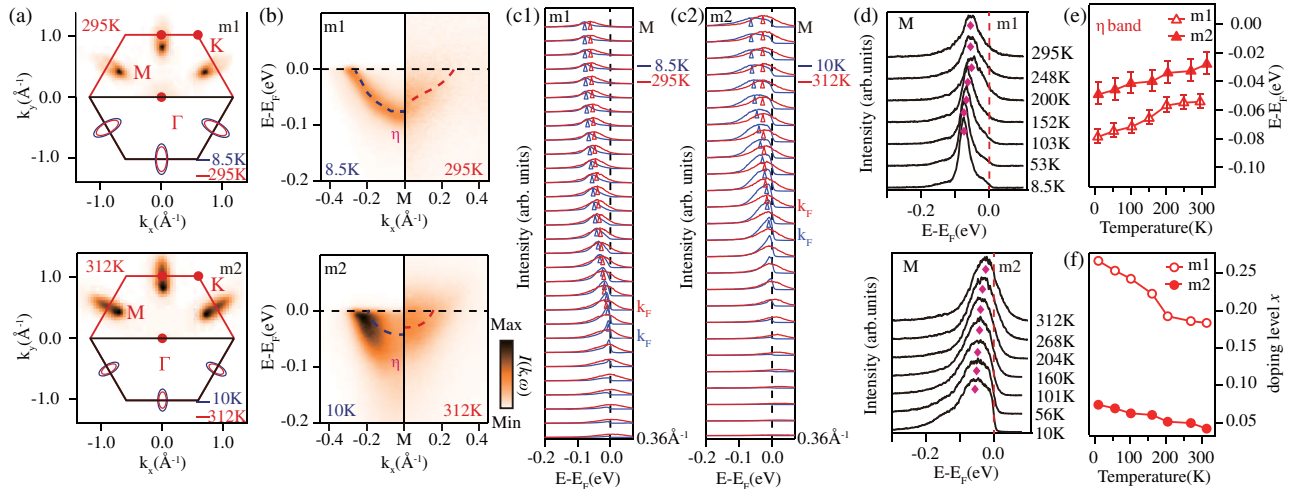

FIG. 3. (a) Fermi surfaces of $(PbSe)_{1.16}(TiSe_2)_m$ ($m = 1, 2$). The upper halves are room-temperature photoemission intensity maps of $m1$ and $m2$ integrated over $(E_F - 2.5 \text{ meV}, E_F + 2.5 \text{ meV})$. Data were sixfold symmetrized. The lower halves are a quantitative comparison of Fermi pocket size at low (8.5 and 10 K) and room (295 and 312 K) temperatures. (b) Comparisons of photoemission intensity plots around M for $m1$ and $m2$ at low and ambient temperatures. ($c1 - c2$) Direct comparisons of the EDCs taken at high and low temperatures for $m1$ and $m2$, respectively. (d) Temperature-dependent EDCs located at M for $m1$ and $m2$, respectively. (e) Temperature dependence of the η band bottom energy for $m1$ and $m2$. (f) Temperature dependence of carrier concentrations for $m1$ and $m2$ due to charge transfer.
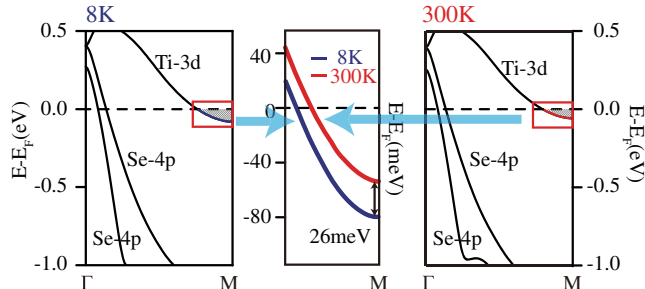
FIG. 4. Band structure comparison of the TiSe$_2$ component in misfit VDWHs at low and room temperatures, as simulated by first-principles calculations based on the thermal expansion of the lattice.

effect of the TiSe$_2$ lattice and then estimated the Ti 3d band shift through band structure calculations (Fig. 4) [42]. This band energy shift is calculated to be about 26 meV from 8 to 300 K, in good agreement with our experimental results (see Supplemental Material [19] for details of this calculation). Since the chemical potential of PbSe lies higher in energy than the Fermi level of TiSe$_2$ [43] and the upward shift of the Ti 3d band observed on warming in misfit VDWHs would reduce the energy gap between them, the electron transfer from PbSe to TiSe$_2$ is effectively suppressed. Accordingly, the resulting carrier concentrations of $m1$ and $m2$ are modulated by as much as 30% and 40%, respectively, by temperature [Fig. 3(f)]. Currently, most prototype devices based on VDWHs are designed mainly according to their low-temperature properties, but are intended to be employed in a room-temperature environment. If such a huge variation in carrier concentration with temperature occurs more generally in VDWHs, it is essential that it should be taken into account.

To summarize, we have comprehensively characterized the electronic structure of the typical naturally occurring VDWHs (PbSe)$_{1.16}$(TiSe$_2$)$_m$ ($m = 1, 2$). By varying the thickness of the TiSe$_2$ layers, we can realize carrier concentration modulation of these VDWHs on an unprecedentedly large scale. Simultaneously, the EPC strength in these VDWHs can be tuned via charge transfer, and thus the domelike dependence of the superconducting transition temperature with carrier concentration in electron-doped TiSe$_2$ can be understood. Most remarkably, a dramatic temperature-dependent band shift is revealed that cuts the carrier concentration nearly in half on warming to room temperature. These findings may provide crucial feedback for the application of devices based on VDWHs and offer a new direction to further our understanding of this interesting class of materials.

[*] dwshen@mail.sim.ac.cn

[1] A. K. Geim and I. V. Grigorieva, Nature (London) **499**, 419 (2013).

[2] D. Jariwala, V. K. Sangwan, L. J. Lauhon, T. J. Marks, and M. C. Hersam, ACS Nano **8**, 1102 (2014).

[3] X. Cui, G. Lee, Y. D. Kim, G. Arefe, P. Y. Huang, C. Lee, D. A. Chenet, X. Zhang, L. Wang, F. Ye, F. Pizzocchero, B. S. Jessen, K. Watanabe, T. Taniguchi, D. A. Muller, T. Low, P. Kim, and J. Hone, Nat. Nanotechnol. **10**, 534 (2015).

[4] K. S. Novoselov, A. Mishchenko, A. Carvalho, and A. H. Castro Neto, Science **353**, aac9439 (2016).

[5] J. E. Padilha, A. Fazzio, and A. J. R. da Silva, Phys. Rev. Lett. **114**, 066803 (2015).

[6] P. Rivera, K. L. Seyler, H. Yu, J. R. Schaibley, J. Yan, D. G. Mandrus, W. Yao, and X. Xu, Science **351**, 688 (2016).

[7] B. Hunt, J. D. Sanchez-Yamagishi, A. F. Young, M. Yankowitz, B. J. LeRoy, K. Watanabe, T. Taniguchi, P. Moon, M. Koshino, P. Jarillo-Herrero, and R. C. Ashoori, Science **340**, 1427 (2013).

[8] C. R. Dean, L. Wang, P. Maher, C. Forsythe, F. Ghahari, Y. Gao, J. Katoch, M. Ishigami, P. Moon, M. Koshino, T. Taniguchi, K. Watanabe, K. L. Shepard, J. Hone, and P. Kim, Nature (London) **497**, 598 (2013).

[9] A. Tsukazaki, S. Akasaka, K. Nakahara, Y. Ohno, H. Ohno, D. Maryenko, A. Ohtomo, and M. Kawasaki, Nat. Mater. **9**, 889 (2010).

[10] X. Du, I. Skachko, F. Duerr, A. Luican, and E. Y. Andrei, Nature (London) **462**, 192 (2009).

[11] C. Lee, G. Lee, A. M. van der Zande, W. Chen, Y. Li, M. Han, X. Cui, G. Arefe, C. Nuckolls, T. F. Heinz, J. Guo, J. Hone, and P. Kim, Nat. Nanotechnol. **9**, 676 (2014).

[12] G. Wiegers, Prog. Solid State Chem. **24**, 1 (1996).

[13] G. Wiegers and A. Meerschaut, J. Alloys Compd. **178**, 351 (1992).

[14] J. Rouxel, A. Meerschaut, and G. Wiegers, J. Alloys Compd. **229**, 144 (1995).

[15] A. J. Molina-Mendoza, E. Giovanelli, W. S. Paz, M. A. Niño, J. O. Island, C. Evangeli, L. Aballe, M. Foerster, H. S. J. van der Zant, G. Rubio-Bollinger, N. Agraït, J. J. Palacios, E. M. Pérez, and A. Castellanos-Gomez, Nat. Commun. **8**, 14409 (2017).

[16] M. Velický, P. S. Toth, A. M. Rakowski, A. P. Rooney, A. Kozikov, C. R. Woods, A. Mishchenko, L. Fumagalli, J. Yin, V. Zlyomi, T. Georgiou, S. J. Haigh, K. S. Novoselov, and R. A. W. Dryfe, Nat. Commun. **8**, 14410 (2017).

[17] D. Merrill, D. Moore, S. Bauers, M. Falmbigl, and D. Johnson, Materials **8**, 2000 (2015).

[18] N. Z. Wang, S. F. Yuan, R. Cong, X. F. Lu, F. B. Meng, C. Shang, and X. H. Chen, Europhys. Lett. **112**, 67007 (2015).

[19] See Supplemental Material http://link.aps.org/supplemental/10.1103/PhysRevLett.120.106401 for more details on experiments, data analysis, and calculations.

[20] G. Kresse and D. Joubert, Phys. Rev. B 59, 1758 (1999).

[21] G. Kresse and J. Furthmller, Comput. Mater. Sci. 6, 15 (1996).

[22] J. P. Perdew, K. Burke, and M. Ernzerhof, Phys. Rev. Lett. 77, 3865 (1996).

[23] D. D. Koelling and B. N. Harmon, J. Phys. C 10, 3107 (1977).

[24] P. Chen, Y. H. Chan, X. Y. Fang, Y. Zhang, M. Y. Chou, S. K. Mo, Z. Hussain, A. V. Fedorov, and T. C. Chiang, Nat. Commun. 6, 8943 (2015).

[25] J. M. Luttinger and J. C. Ward, Phys. Rev. 118, 1417 (1960).

[26] N. Nakagawa, H. Y. Hwang, and D. A. Muller, Nat. Mater. 5, 204 (2006).

[27] X. H. Niu, R. Peng, H. C. Xu, Y. J. Yan, J. Jiang, D. F. Xu, T. L. Yu, Q. Song, Z. C. Huang, Y. X. Wang, B. P. Xie, X. F. Lu, N. Z. Wang, X. H. Chen, Z. Sun, and D. L. Feng, Phys. Rev. B 92, 060504 (2015).

[28] R. Peng, H. C. Xu, M. Xia, J. F. Zhao, X. Xie, D. F. Xu, B. P. Xie, and D. L. Feng, Appl. Phys. Lett. 104, 081606 (2014).

[29] J. H. Davies, The Physics of Low-Dimensional Semiconductors: An Introduction (Cambridge University Press, Cambridge, 1997).

[30] T. E. Kidd, T. Miller, M. Y. Chou, and T.-C. Chiang, Phys. Rev. Lett. 88, 226402 (2002).

[31] P. Aebi, T. Pillo, H. Berger, and F. Lévy, J. Electron Spectrosc. Relat. Phenom. 117–118, 433 (2001).

[32] J. F. Zhao, H. W. Ou, G. Wu, B. P. Xie, Y. Zhang, D. W. Shen, J. Wei, L. X. Yang, J. K. Dong, M. Arita, H. Namatame, M. Taniguchi, X. H. Chen, and D. L. Feng, Phys. Rev. Lett. 99, 146401 (2007).

[33] E. Morosan, H. W. Zandbergen, B. S. Dennis, J. W. G. Bos, Y. Onose, T. Klimczuk, A. P. Ramirez, N. P. Ong, and R. J. Cava, Nat. Phys. 2, 544 (2006).

[34] H. W. Ou, J. F. Zhao, Y. Zhang, B. P. Xie, D. W. Shen, Y. Zhu, Z. Q. Yang, J. G. Che, X. G. Luo, X. H. Chen, M. Arita, K. Shimada, H. Namatame, M. Taniguchi, C. M. Cheng, K. D. Tsuei, and D. L. Feng, Phys. Rev. Lett. 102, 026806 (2009).

[35] P. Chen, Y. H. Chan, X. Y. Fang, S. K. Mo, Z. Hussain, A. V. Fedorov, M. Y. Chou, and T. C. Chiang, Sci. Rep. 6, 37910 (2016).

[36] L. Perfetti, H. Berger, A. Reginelli, L. Degiorgi, H. Höchst, J. Voit, G. Margaritondo, and M. Grioni, Phys. Rev. Lett. 87, 216404 (2001).

[37] F. Caruso, H. Lambert, and F. Giustino, Phys. Rev. Lett. 114, 146404 (2015).

[38] Y. Liu, D. F. Shao, L. J. Li, W. J. Lu, X. D. Zhu, P. Tong, R. C. Xiao, L. S. Ling, C. Y. Xi, L. Pi, H. F. Tian, H. X. Yang, J. Q. Li, W. H. Song, X. B. Zhu, and Y. P. Sun, Phys. Rev. B 94, 045131 (2016).

[39] P. Giannozzi et al., J. Phys. Condens. Matter 21, 395502 (2009).

[40] J. P. Perdew and A. Zunger, Phys. Rev. B 23, 5048 (1981).

[41] P. B. Allen and R. C. Dynes, Phys. Rev. B 12, 905 (1975).

[42] S. L. Budko, P. C. Canfield, E. Morosan, R. J. Cava, and G. M. Schmiedeshoff, J. Phys. Condens. Matter 19, 176230 (2007).

[43] D. R. Merrill, D. B. Moore, S. R. Bauers, M. Falmbigl, and D. C. Johnson, Materials 8, 2000 (2015).